Static path approximation in deformed nuclei

B. Lauritzen
NORDITA, Copenhagen, Denmark
G. Bertsch
Department of Physics and Cyclotron Laboratory, Michigan State University, East Lansing, Michigan 48824
(Received 23 December 1988)

The static path approximation to the partition function of a nucleus is studied for Hamiltonians with quadrupole-quadrupole interactions. The static path approximation yields a higher level density than the finite-temperature Hartree theory due to a better treatment of the deformation degrees of freedom. The level density is further increased when the nucleus has a static deformation. Comparing with the exact partition function of the Elliott SU(3) model, the static path approximation is found to be remarkably accurate and far superior to finite-temperature Hartree theory.

I. INTRODUCTION

We have recently suggested that the statistical mechanics of nuclei might be better described by a certain approximation in a functional integral formulation than by the conventional finite-temperature Hartree-Fock theory;[1,2] see also Ref. 3. The functional integral we employ is the Hubbard-Stratonovich representation of the partition function, which is a path integral in the space of single-particle potential fields. The approximation, introduced to condensed matter physics in Ref. 4, is to integrate only over static potential fields; we call this the static path approximation (SPA). It makes a tractable theory for dealing with the hundred or so particles that constitute a nucleus, provided the residual interaction is represented by a few separable terms. The computational difficulty would only be somewhat larger than required for systematic finite-temperature Hartree calculations, but since this is already large it is important to test the static path approximation on simplified models before proceeding with the numerical program.

In our previous work we investigated the theory using a pairing Hamiltonian, and found very encouraging results. Deformations and rotational degrees of freedom are also an important aspect of nuclear dynamics, and in this work we want to see how they affect the statistical properties of nuclei. Empirically, deformed nuclei exhibit higher level densities due to the rotational degrees of freedom:[5,6] We will show in the next section qualitatively how this enhancement emerges from the path-integral formulation. It will also be shown that the SPA level density is higher than that of Hartree theory even when the nucleus is spherical.

In order to test the approximation, it is necessary to compare with a model that can be exactly solved. The partition function for Elliot's SU(3) model[7] can be evaluated for various shells of interest, and we use this as our testing ground. The details are presented in the third section. We find that the static path approximation describes the level density very well, unlike the Hartree approximation, which we also consider for comparison purposes. However, the static path approximation does not produce the lowest part of the energy spectrum. This is the major effect of the truncation of the paths, that the highly correlated low states are effectively absent from the partition function.

In Sec. IV we apply the SPA to a more realistic Hamiltonian, with single-particle wave functions and energies appropriate for the $A\sim 60$ mass region. This demonstrates the feasibility of the method for a more realistic situation than we could achieve with the SU(3) model, where the single-particle levels are all degenerate. We also find here that the level density in SPA is much higher than in Hartree theory.

II. SPA FOR THE QUADRUPOLE HAMILTONIAN

We believe that a Hamiltonian whose interaction part is of the pairing-plus-quadrupole type can be realistic enough to describe the level densities. We write this as

$$H = H_0 - \tfrac{1}{2}\chi Q\cdot Q^{\dagger} - GP^{\dagger}P \ . \tag{1}$$

Here Q is a quadrupolar single-particle operator and P is the operator annihilating a pair of particles. H_0 is the single-particle Hamiltonian, which would be determined from the single-particle spectrum of a realistic potential well. The partition function is expressed as a functional integral over the amplitudes of the pairing field and of the five components of the quadrupole field. The static path approximation to the integral is given by the following:[2]

$$Z(\mu,T)=\frac{4\pi}{GT}\left[\frac{a}{2\pi T}\right]^{5/2}\int_0^{\infty}\Delta\, d\Delta\int_0^{\pi}d\psi\int_0^{\pi}d\theta\sin\theta\int_0^{\infty}\beta^4\, d\beta\int_0^{\pi/3}d\gamma\sin(3\gamma)\exp\left[-\frac{a\beta^2}{2T}-\frac{\Delta^2}{GT}\right]$$
$$\times\,\mathrm{tr}\left\{\exp\left[-\frac{H'(\beta,\gamma,\Delta)}{T}\right]\right\}, \tag{2}$$

where

$$H'(\beta,\gamma,\Delta)=H_0-M\omega_0^2\beta r^2\left[\cos\gamma\ Y_{20}+\sin\gamma\ \frac{1}{\sqrt{2}}(Y_{2,2}+Y_{2,-2})\right]-GP_0-\Delta(P^\dagger+P)-\lambda N$$

and

$$a=\frac{M^2\omega_0^4}{\chi}\ .$$

In this equation β and γ are the usual deformation parameters, ψ and θ are orientation angles, and Δ is the pairing gap. Also M is the mass of a nucleon and ω_0 is the oscillator frequency for the orbitals.

The role of deformation can be seen qualitatively by evaluating the integral with some analytically tractable approximation to the integrand. For this purpose we only consider the single-particle and quadrupole-quadrupole terms of the Hamiltonian (1). The integrand is independent of orientation in the absence of external fields, so the two angular integrations can be performed immediately. We also anticipate a mild dependence on axial asymmetry γ to integrate out this variable. The remaining dependence on β and T is conveniently expressed by defining a free-energy-like quantity $F(\beta,T)$:

$$\exp\left[-\frac{a\beta^2}{2T}\right]\mathrm{tr}\{\exp[-H'(\beta)/T]\}=\exp[-F(\beta,T)/T]\ . \quad (3)$$

We now assume that F can be expanded in powers of β to write

$$F(\beta,T)=c_0(T)+\tfrac{1}{2}c_2(T)(\beta-\beta_0)^2\ .$$

Here β_0 is a constant giving the static deformation in Hartree theory. The integration can be done easily in two limiting cases, $\beta_0=0$ and $\beta_0\gg\sqrt{T/c_2}$. In the first case, the partition function becomes

$$Z_{\mathrm{sph}}(T)=\left[\frac{a}{c_2}\right]^{5/2}\exp(-c_0/T)\ . \quad (4)$$

This is to be compared with the partition function in the Hartree theory, which is simply

$$Z_H=\exp(-c_0/T)\ . \quad (5)$$

Thus the static path partition function differs from the Hartree one by a prefactor, even in the case when the solution is spherical.

It is interesting to examine more closely the origin and magnitude of this factor. The level density is given by the inverse Laplace transform of Z and will effectively contain the same factor. We expect more states with the static path approximation because the nucleus is not fixed at a given deformation. The extra low-lying states are not well described by single-particle excitations within a fixed Hartree field, but require shape changes and rearrangement of the particles to make a low state in the new field. The softer the nucleus is to deformations, the larger will be this effect. To estimate the effect quantitatively, we use a somewhat more realistic quadrupole interaction than the multipole interaction of Eq. (1). The self-consistent surface response in the semi-infinite slab model is given by[8]

$$v(r,r')=-\kappa\frac{dU}{dr}\bigg|_r\frac{dU}{dr}\bigg|_{r'}\delta^{(2)}(r_{\mathrm{perp}}-r'_{\mathrm{perp}})\ , \quad (6)$$

where $\kappa\sim0.63\ \mathrm{MeV}^{-1}\,\mathrm{fm}^4$. Here U is the static mean-field potential. The quadrupole component of the self-consistent surface interaction is extracted by replacing the semi-infinite geometry with a spherical surface, substituting for the transverse delta function,

$$\delta^{(2)}(r_{\mathrm{perp}}-r'_{\mathrm{perp}})\sim R^{-2}\delta^{(2)}(\Omega-\Omega')\sim R^{-2}\sum_L Y_L\cdot Y_L^*\ .$$

With the above interaction, the integrand in the static path integral is

$$\exp\left[-\frac{1}{2}\frac{R^4}{\kappa T}\beta^2\right]\mathrm{tr}\{\exp[-H(\beta,\gamma)/T]\}\ , \quad (7)$$

where $H(\beta,\gamma)$ is given by Eq. (17). Thus the coefficient a in Eq. (4) becomes $a=R^4/\kappa$. The other constant c_2 can only be determined by a systematic mapping of the potential energy surface. However, except for kinetic contributions to the stiffness parameter, the result averaged over many nuclei should match the liquid drop deformation potential. This is given by[9] $c_2=4R^2\sigma$ where $\sigma\sim1$ MeV/fm^2 is the surface tension, and the Coulomb interaction has been neglected. The ratio of partition functions is then found to be

$$\frac{Z_{\mathrm{sph}}}{Z_H}=\left[\frac{R^2}{4\kappa\sigma}\right]^{5/2}\sim0.25A^{5/3}\ . \quad (8)$$

Thus we find a large increase in the partition function associated with the shape fluctuations of a spherical nucleus. The effect grows with the size of the nucleus, because the liquid drop energetics allow more states for a given energy cost in a large system.

We next examine the partition function for deformed nuclei. When the static deformation is large, the β integration is approximated as

$$\int_0^\infty\beta^4\,d\beta\sim\beta_0^4\int_{-\infty}^{\infty}d(\beta-\beta_0)\ ,$$

yielding for the partition function

$$Z_{\mathrm{def}}=\frac{2}{3}\left[\frac{a}{c_2}\right]^{5/2}\left[\frac{c_2\beta_0^2}{T}\right]^2\exp(-c_0/T)\ . \quad (9)$$

The exponential factor is the same as in the other limits, and the only difference is in the prefactor. This prefactor is not well behaved; the T dependence leads to a negative heat capacity in the limit where $T\to0$. This was noted also in Ref. 2; when the maxima of the integrand form an n-dimensional surface in the space of deformation vari-

ables, the prefactor diverges as $T^{-n/2}$ for $T\to 0$. In the present case, four of the five deformation coordinates are cyclic, producing the power T^{-2}. As a practical matter, the heat capacity becomes negative only at the lowest temperatures. Despite the pathology, we will see later that the partition function is quite accurate above the lowest temperatures.

The peculiar T dependence when the free energy is independent of a coordinate is probably an intrinsic limitation of the static path approximation that should have been expected. When a variable becomes free, i.e., no longer affects the integrand, then classically there is an infinite degeneracy of states in that degree of freedom. If one were to make an improved treatment of the partition function, one would find a kinetic energy associated with that degree of freedom. The classical partition function associated with a kinetic energy $p^2/2m$ is $(2\pi mT)^{1/2}$. This would introduce a factor $T^{1/2}$ canceling the singular T dependence of the static path approximation. Although this argument seems quite plausible, we have been unable to show how an approximation beyond the static path would restore the correct temperature dependence.

We conclude this section with a numerical estimate of the deformed nucleus enhancement. In general, the deformed partition function is enhanced over the spherical by a factor $(c_2\beta_0^2/T)^{1/2}$ for each collective degree of freedom in which there is no restoring force. For axially symmetric nuclei which can rotate freely in only two out of the three Euler angles, the enhancement is given by

$$\frac{Z_{\rm def}}{Z_{\rm sph}}\sim\frac{c_2\beta_0^2}{T}\ . \tag{10}$$

We evaluate this with the following parameters: $T\sim 0.5$ MeV; $\beta_0\sim 0.3$; and $c_2\sim 70$ MeV, which is appropriate for $A\sim 150$ (Ref. 10). This yields $Z_{\rm def}/Z_{\rm sph}\sim 12.5$. The value should be compared to the enhancement of the level density by a factor $\sigma_K^2\sim 35$, as discussed in Ref. 6. Here σ_K measures the fluctuation of the K-quantum numbers and increases with the temperature as $\sigma_K\sim T^{1/2}$, a result much different from the form of Eq. (10). Of course, until the temperature dependence is better understood, no conclusion can be drawn from this comparison.

III. EXACT SOLUTION

From the simple parametrization of the free energy $F(\beta,\gamma)$ above, it was shown how deformation leads to an increased level density. This is to be expected for a theory that includes the collective rotational degrees of freedom. In order to test the static path approximation quantitatively we consider in the following Elliot's SU(3) model,[7] which is known to generate rotational motion.

The exact energy spectrum of the quadrupole-quadrupole interaction may be obtained using group theoretical methods. We write, for the Hamiltonian,

$$H_Q=-\tfrac{1}{2}\chi Q\cdot Q^{\dagger},\quad Q_\mu=r^2Y_{2\mu}\ , \tag{11}$$

and restrict ourselves to a single harmonic oscillator shell. The single-particle energies are degenerate in the shell and the many-particle wave functions can be classified according to the irreducible representations of SU(3). The eight generators of unimodular unitary transformations in three dimensions are given by the five quadrupole operators $Q_{\mu,\Delta N=0}$ together with the angular momentum operators L_k. The irreducible representations of the group are labeled by two numbers (λ,μ) and the states in each representation (λ,μ) may be classified according either to the eigenvalues of L_0 and L^2 or to the eigenvalues of L_0 and Q_0.

Since the Hamiltonian (11) may be combined with L^2 to form the second-order Casimir operator of the group, the first classification is convenient for evaluating the exact energy spectrum,[11]

$$E_Q=-\tfrac{1}{2}\chi q^2[\lambda^2+\mu^2+\lambda\mu+3(\lambda+\mu)-\tfrac{3}{4}L(L+1)]\ ,$$
$$q=\left[\frac{5}{4\pi}\right]^{1/2}\frac{\hbar}{M\omega_0}\ . \tag{12}$$

The quadrupole Hamiltonian (11) is seen to generate rotational motion, and the coefficient in front of the angular momentum in (12) is given by the rigid-body value of the moment of inertia, when self-consistency between deformation and potential is required. In the calculations presented, we use the value

$$\tfrac{1}{2}\chi q^2=X_{\rm ren}35.8A^{-5/3}\ \text{MeV},\quad A=\tfrac{2}{3}(N_{\rm sh}+\tfrac{3}{2})^3 \tag{13}$$

which takes into account the polarization of the core. A renormalization factor $X_{\rm ren}$ is introduced, which is equal to 1 when both protons and neutrons are considered and equal to 2 when only one kind of particles is present.

In a given oscillator shell of s spatial dimensions, the many-body states are characterized by the irreducible representations $[f]$ of U_s, the group of unitary transformations in s dimensions. The partition $[f]$ denotes the particle symmetry, and the evaluation of the energy spectrum amounts to a decomposition of $[f]$ into the SU(3) classifications, $U_s\supset$SU(3). For this we have used a code by Draayer.[12] The decomposition of the (λ,μ) set into eigenvalues of L_0 and L^2 is given in Ref. 7. Finally, the spin-isospin wave functions are formed that produce totally antisymmetric states when combined with the spatial wave functions.

The second classification of (λ,μ) in terms of L_0 and Q_0 is useful for calculating the Hartree approximation to the ground state. For this classification a third quantum number (Λ) is required to uniquely determine the state. In each representation (λ,μ) the eigenvalues of Q_0 are given by

$$\langle Q_0\rangle=\tfrac{1}{2}qe,\quad e=2\lambda+\mu,2\lambda+\mu-3,\ldots,-\lambda-2\mu\ . \tag{14}$$

When the nucleus is axially symmetric, the Hartree approximation to the ground state of the Hamiltonian (11) is then obtained from the maximum value of $\langle Q_0\rangle$,

$$E_H=-\tfrac{1}{2}\chi\langle Q_0\rangle^2=-\tfrac{1}{2}\chi q^2(\lambda^2+\tfrac{1}{4}\mu^2+\lambda\mu)_{\rm max}\ . \tag{15}$$

This energy lacks the linear terms in λ,μ as compared to the exact ground-state energy (16). Since the maximum values of λ and μ increase rapidly with the particle num-

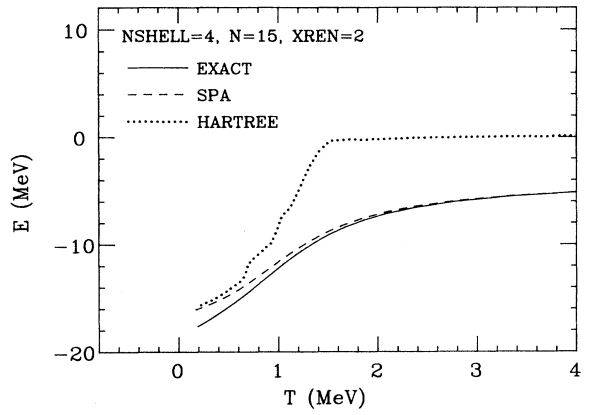

FIG. 1. Energetics of the Elliott SU(3) Hamiltonian, for 15 particles in the *gds* major shell. The solid line shows the expectation of the energy as a function of temperature from the exact solution of the SU(3) Hamiltonian. The dashed and dotted lines show the SPA and the Hartree approximation, respectively. Note the pronounced phase transition in the Hartree theory, which is completely absent in the true Hamiltonian or the SPA.

ber in the shell, the Hartree result (15) is a good approximation only for large shells. The static path approximation to the ground state does no better that the Hartree approximation and consequently does not give the correct energy.

For our numerical comparison of the different treatments of the SU(3) Hamiltonian, we shall consider 15 particles in the $0g$-$1d$-$2s$ major shell. For technical reasons, we consider states of one kind of particle only, so that the permutation partition has at most two rows. The dimensionality of the space is $2^{30}\sim 10^9$ many-particle states of the grand canonical ensemble. The results are summarized in Figs. 1 and 2. Figure 1 shows the energy as a function of temperature. The Hartree theory shows an abrupt change in the specific heat at $T\sim 1.5$ MeV, which is the phase transition from deformed to spherical. In contrast, the actual energy varies quite smoothly as a function of temperature—there is not even a hint of a phase transition. The SPA reproduces the actual behavior very well. The level density is calculated from the partition function using the saddle-point approximation to the inverse Laplace transform, as described in the next section. There is similarly excellent agreement between the SPA and the level density from the exact partition

TABLE I. Neutron levels in the nucleus ^{64}Zn, determined as eigenfunctions of the Hamiltonian (16), with parameters $V_0=-50$ MeV, $V_{ls}=-15$ MeV fm$^2\hbar^{-2}$, $a=0.65$ fm, and $r_0=1.25$ fm.

Level	Energy (MeV)
$1p_{3/2}$	−10.2
$1p_{1/2}$	−8.3
$0f_{7/2}$	−14.2
$0f_{5/2}$	−8.8
$0g_{9/2}$	−4.4

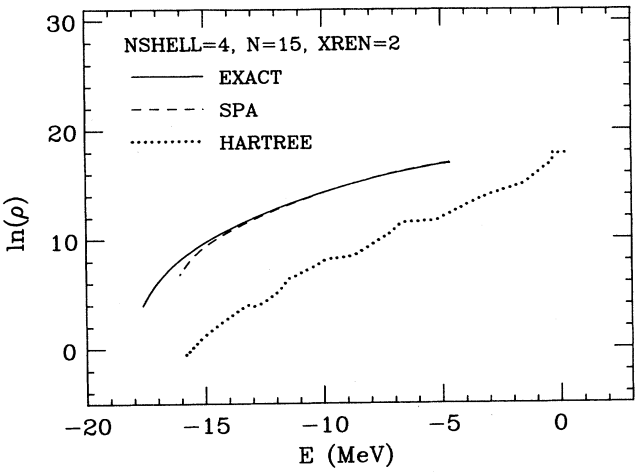

FIG. 2. Level densities for the Elliott SU(3) Hamiltonian, as in Fig. 1. The SPA is seen to be far superior to Hartree, provided the absolute energy scale is established.

function, which may be seen from Fig. 2. Again, the Hartree theory has far too low a level density.

However, the good agreement between SPA and the exact level density only extends over the region of energies in which states are obtained. Thus, the region within 2 MeV of the ground state is incorrectly described by either SPA or Hartree theory. The sources of the additional correlation energy in the ground state are discussed in the Appendix.

IV. A NUMERICAL EXAMPLE

In this section we will illustrate the technique calculating the level density of the nucleus ^{64}Zn. The single-particle Hamiltonian is determined from a Woods-Saxon

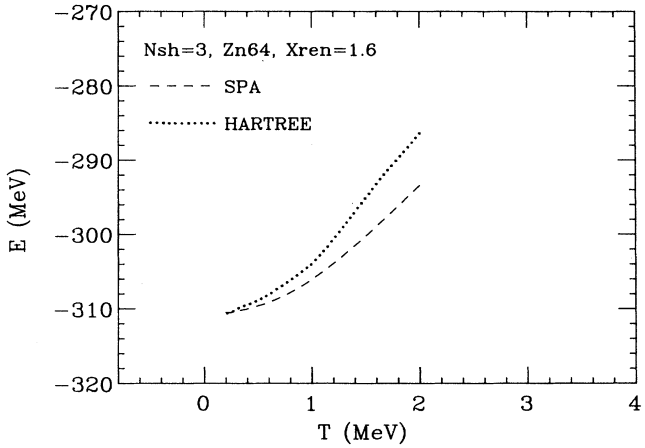

FIG. 3. Comparison of the static path and Hartree approximations for the pairing-plus-quadrupole Hamiltonian with realistic single-particle energies. The Hartree and SPA agree at low temperatures, since the Hartree minimum dominates the integrand in the SPA integration. Note that the Hartree energy increases more rapidly with temperature than does the SPA energy.

potential of standard form,

$$H_0=\frac{p^2}{2m}+V_0 f(x)+V_{ls}\sigma\cdot l f'(x)/ar \ , \tag{16}$$

where $f(x)=1/[1+\exp(x)]$ and $x=(r-r_0A^{1/3})/a$. The well parameters and single-particle eigenvalues are quoted in Table I.

We take the residual interaction to be of the surface coupling form (6) rather than a pure multipole. To take into account the polarization of the core, the interaction strength has been renormalized by a factor 1.6. In this preliminary study, we drop the pairing term in Eq. (1). The single-particle Hamiltonian is then given by

$$H(\beta,\gamma)=H_0-\beta R\frac{dU}{dr}[\cos\gamma\ Y_{20} +\sin\gamma\,(Y_{22}+Y_{2,-2})/\sqrt{2}] \ . \tag{17}$$

The first step in the evaluation of the Hubbard-Stratonovich integral is to diagonalize the deformed single-particle Hamiltonian on a grid points in the (β,γ) plane. The trace in Eq. (2) is then evaluated over an additional grid of points in the temperature and the two chemical potentials for protons and neutrons, according to the formula

$$\mathrm{tr}\{\exp\{-[H(\beta,\gamma)-\mu_n N-\mu_p Z]/T\}\} = \prod_{I,\zeta=n,p}(1+e^{-[\epsilon(\beta,\gamma)-\mu_\zeta]/T}) \ , \tag{18}$$

where the index i ranges over the single-particle eigenvalues. The integral for the partition function is now performed numerically over the mesh in the (β,γ) plane.

The energy as a function of temperature is determined from the numerical differentiation,

$$E(T)=-\frac{d\ln Z}{d(1/T)}+\mu_n N+\mu_p Z \ . \tag{19}$$

In the same way, the chemical potentials for neutrons and protons are determined from the relations

$$Z,N=T\frac{d\ln Z}{d\mu_{p,n}} \ .$$

The quantity of most direct interest is the level density as a function of energy. The level density is evaluated from the inverse Laplace transform of the partition function. We use the saddle-point approximation here to obtain the formula

$$\rho(N_p,N_n,E)=\frac{Z(\mu_p,\mu_n,1/T)\exp[(E-\mu_p Z-\mu_n N)/T]}{(2\pi)^{3/2}D^{1/2}} \ , \tag{20}$$

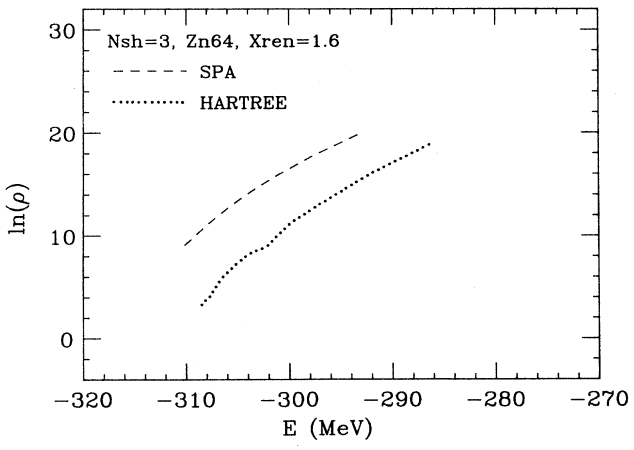

FIG. 4. Level densities in the ^{64}Zn example. The major difference is a higher level density in the SPA. This is essentially explained by Eqs. (4) and (5).

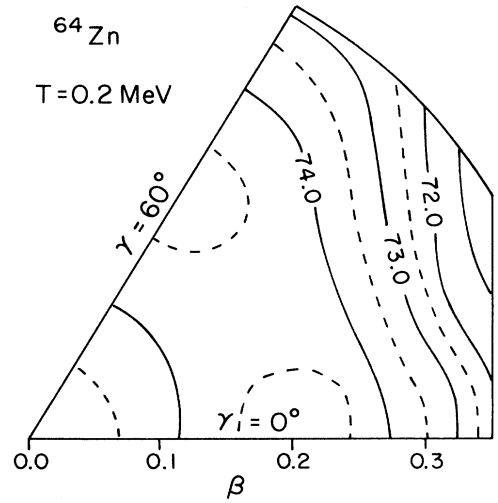

FIG. 5. Free-energy surface for the ^{64}Zn example, at a temperature of 0.2 MeV. Contours are shown at 1-MeV intervals. There is a broad minimum at $\beta\sim0.2$ which is very soft in the γ degree of freedom.

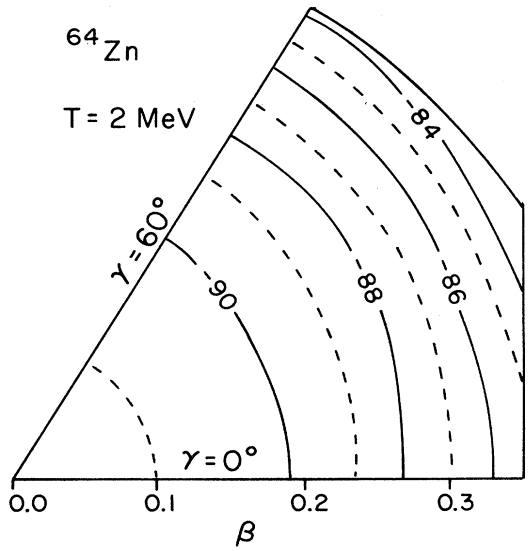

FIG. 6. Free-energy surface as above, with the temperature increased to 2 MeV. The minimum has now moved to the spherical shape.

where D is the 3×3 determinant of the second derivative matrix

$$\frac{d^2Z(x)}{dx_i dx_j} ,$$

with $x=(1/T,\mu_p/T,\mu_n/T)$.

The results for ^{64}Zn are shown in Figs. 3–6. The calculations were done using a grid with mesh points separated in β by 0.05. Figure 3 shows the relation between energy and temperature, comparing the SPA with finite-temperature Hartree theory. Both theories have identical energies at zero temperature. The actual energy of the system is, of course, lower because correlations are neglected. The Hartree energy increases more rapidly with temperature than the SPA energy. This higher specific heat is an indication of the more pronounced phase transition in Hartree theory. In Fig. 4 we show the corresponding level density, as calculated from Eq. (20). The level density in the SPA is higher by a factor of 50–1000. This confirms the qualitative argument presented earlier, that the prefactor in the level density would be much higher.

Figures 5 and 6 show contours of the free energy F from Eq. (3), in the (β,γ) plane. In Fig. 5, the contours are shown for a temperature of 0.2 MeV. Here the Hartree state is deformed, and the free-energy surface is seen to be rather soft in the γ degree of freedom. The surface at a temperature of 2 MeV is shown in Fig. 6. The minimum has moved to a spherical shape, thus in Hartree theory a phase transition has occurred. These contour plots may be used to obtain the free-energy stiffness c_2, which comes out to be somewhat larger than the liquid drop stiffness used in the estimate (8). The lack of agreement could arise from a number of sources, for example an inadequate model space or incorrect renormalization factor.

V. CONCLUSION

Our study with ^{64}Zn demonstrates the technical feasibility of using the SPA in Hamiltonians with realistic single-particle energies. The comparison of the SPA with the Elliott SU(3) model shows that the approximation is an excellent one, provided the ground-state correlation energy can be estimated by other methods.

The qualitative results of the comparison with the Hartree approximation are twofold. First, there is a much higher level density than Hartree theory predicts. This was expected, and is due to the fact that shape degrees of freedom are soft and their fluctuations are ill treated by Hartree theory. The second result is that Hartree theory predicts much too sharp a phase transition between spherical and deformed shapes. This has been noted earlier using a more phenomenological construction of the free-energy surface.[13,14]

We believe that a global study of nuclear levels densities is now possible, and is warranted by the successful tests of the SPA which we presented here. We hope to continue along this direction.

ACKNOWLEDGMENTS

We thank J. Draayer for providing us with a computer code to find the SU(3) representations of multiparticle states. We would like to acknowledge conversations with P. Arve and S. Levit. This work was supported the Carlsberg Foundation and by the National Science Foundation under Grant 87-14432.

APPENDIX

In Sec. III we demonstrated that the SPA provides an accurate approximation to the nuclear level density at moderate and high excitation energy, but fails close to the ground-state energy. Since level densities are measured as a function of excitation energy, the SPA becomes useful only when the energy shift between the exact ground state and the Hartree ground state is known. In this appendix we examine the origin of the ground-state correlation energy in the framework of the Elliott SU(3) model. In the Elliott model, the ground state may be obtained from the Hartree state by angular momentum projection on $L=0$. The energy shift δE has contributions from the exchange term neglected in evaluating the Hartree energy and from the average rotational energy of the deformed state,

$$\delta E=\delta E_F+\delta E_L . \tag{21}$$

The rotational energy is given by

$$\delta E_L=\frac{1}{2J}\langle\Psi|L^2|\Psi\rangle , \tag{22}$$

where J denotes the moment of inertia. The moment of inertia can be estimated as the average value for the ground-state band or may be calculated for the Hartree ground state. In the SU(3) model it is found that the rotational contribution is responsible for half of the energy shift, $E_L=\frac{1}{2}\delta E$, while the second half is given by the exchange energy. Thus, in more realistic models, we expect that roughly half of δE can be estimated by straightforward projection techniques.

When the pairing interaction is included in the Hamiltonian, the energy shift includes effects of particle-number nonconservation. The mean-field ground state is equivalent to the one obtained in a Hartree-Bogoliubov calculation, and the energy shift may be obtained by carrying out angular momentum and particle-number projections.

[1]P. Arve, G. Bertsch, B. Lauritzen, and G. Puddu, Ann. Phys. (N.Y.) **183**, 309 (1988).

[2]B. Lauritzen, P. Arve, and G. Bertsch, Phys. Rev. Lett. **61**, 2835 (1988).

[3]Y. Alhassid and J. Zingman, Phys. Rev. C **30**, 684 (1984).

[4]W. Evenson, J. Schrieffer, and S. Wang, J. Appl. Phys. **41**, 1199 (1970).

[5]S. Bjørnholm, A. Bohr, and B. R. Mottelson, *Physics and*

Chemistry of Fission (IAEA, Vienna, 1974), Vol. I, p. 367.
[6]A. Bohr and B. Mottelson, *Nuclear Structure* (Benjamin, Reading, Mass, 1975), Vol. II, p. 40.
[7]J. P. Elliott, Proc. R. Soc. London, Ser. A **245**, 562 (1958); J. P. Elliott and M. Harvey, *ibid.* **272**, 557 (1963).
[8]H. Esbensen and G. Bertsch, Ann. Phys. (N.Y.) **157**, 255 (1984); G. Bertsch and H. Esbensen, Phys. Lett. **161B**, 248 (1985).
[9]A. Bohr and B. Mottelson, *Nuclear Structure* (Benjamin, Reading, Mass, 1975), Vol. II, p. 658.
[10]A. Bohr and A. Mottelson, *Nuclear Structure* (Benjamin, Reading, Mass., 1975), Vol. II, p. 529.
[11]A. Bohr and B. Mottelson, *Nuclear Structure* (Benjamin, Reading, Mass., 1969), Vol. I, p. 124.
[12]J. Draayer, unpublished.
[13]J. M. Pacheco, C. Yannouleas, and R. A. Broglia, Phys. Rev. Lett. **61**, 294 (1988).
[14]A. Goodman, Phys. Rev. C **37**, 2162 (1988); **38**, 1092 (1988).